JOURNAL OF NANO- AND ELECTRONIC PHYSICS
Vol. **7** No 1, 01012(7pp) (2015)

ЖУРНАЛ НАНО- ТА ЕЛЕКТРОННОЇ ФІЗИКИ
Том **7** № 1, 01012(7cc) (2015)

Charge States of Bare Silicon Clusters up to Si_8 by Non-Conventional Tight-Binding Method

A.P. Mukhtarov, A.B. Normurodov, N.T. Sulaymonov, F.T. Umarova

Institute of Nuclear Physics, 100214 Tashkent, Uzbekistan

(Received 03 December 2014; published online 25 March 2015)

A recently developed non-conventional tight-binding method was applied in combination with molecular dynamics to compute the geometric structures and cohesion energies of small stable pure Si clusters containing from 3 to 8 atoms, in neutral, positive and negative charge states. The influence of the charge state on the cluster configuration and cohesion energy is considered. The Anderson U(-) effect is observed in Si_3-Si_5 clusters. Doubly positively charged states are found to be the most energetically stable form for all clusters considered. The results computed with this semi-empirical approach are compared to predictions from state-of-the-art ab initio methods.

Keywords: Silicon cluster, Non-conventional tight-binding method, Cohesion energy.

PACS numbers: 36.40. – c, 31.10. + z

1. INTRODUCTION

Over the past decade, there has been substantial and growing interest in small silicon clusters, both due to fundamental interest in the physics and chemistry of these prototypical clusters, and due to potential technological applications of somewhat larger silicon nanocrystals, which exhibit efficient photoluminescence. Hydrogenated silicon clusters are known to form during the early stages of silicon nanocrystal synthesis, and play an important role in the nucleation and growth process. In addition, small pure silicon clusters have been attracting research interest because of their fundamental importance in understanding of formation and growth processes of silicon nanoparticles and in understanding the mechanism of photoluminescence in silicon nanocrystals. Several experimental studies of neutral and charged silicon clusters have been published, including measurements of photodetachment of negative ions [1], two-photon ionization [2-3], chemical reactivities [4-8], collision-induced dissociation [9], and photofragmentation [10-12] of the positive and negative ions. In such studies, it has proven very difficult to obtain small clusters of uniform size and structure. For this reason, computer simulations of such clusters are an essential tool to study them, and there have been several detailed calculations carried out by tight-binding [13-14] and ab-initio [15-23] methods. Raghavachari et al. have studied structures and energies of Si_2-Si_6 [24] and Si_7-Si_{10} [22] clusters by ab-initio Hartree-Fock with the polarized 6-31G* basis set. They identified clusters containing four, six, or seven atoms as "magic clusters". They also discussed the hybridization and bonding in small clusters. Negatively charged small silicon clusters Si_n (n = 2-5) have been treated by Curtiss and et al [21] using the Gaussian-2(G2) composite method, based on ab-initio molecular orbital theory. Other charged clusters that can also be formed during nanocrystal synthesis or deposition on a substrate have not been considered before. The relative energies of charged small silicon clusters, their geometrical configurations, and changes in their structure upon change of their charge state are of interest but have not pre-viously been treated comprehensively by a single theoretical method. The present contribution presents such a treatment, using a new computationally inexpensive Non-conventional Tight-Binding Method (NTBM) [25] that can be consistently applied to larger clusters as well. In prior studies, a quasi-one-dimensional growth pattern of nanosilicon [26], a new mechanism of the Staebler-Wronsky effect [27] in amorphous silicon, U-negative behavior of the vacancy in silicon [28] and other reactions [29-30] have been predicted by this method.

In this article we present the results on stable configurations of the small bare silicon clusters included up to 8 silicon atoms in different charge states calculated using our Molecular Dynamic NTBM [25]. The paper is organized as follows: Section 2 summarizes the computational methods used in the present work. In section 3, the ground state geometries and cohesion energies in the different charge states are presented and discussed. Finally we summarize our results in section 4.

2. COMPUTATIONAL DETAILS

Stable configurations of small clusters have been found using a combination of the non-conventional tight-binding (NTB) method with molecular dynamics (MD). NTB provides the interatomic potential. The equilibrium geometry of clusters was optimized by MD.

We use NTB with a total energy functional expression that is different in form from commonly used TB energy functionals. The expression for total energy functional of NTB is written as [25]

$$E_{tot} = \sum_{\mu}\sum_{\nu>\mu}\frac{Z_{\mu}^{scr}Z_{\nu}^{scr}}{R_{\mu\nu}} + \sum_{\mu}\sum_{\nu>\mu}\frac{Q_{\mu}Q_{\nu}}{R_{\mu\nu}} + \sum_{\mu}\sum_{\nu>\mu}\sum_{i}\sum_{j}P_{\mu_i,\nu_j}H_{\mu_i,\nu_j} + \sum_{\mu}E_{\mu} - E_{\mu}^{0}\ , \quad (1)$$

where

$$Z_\mu^{scr} = Z_\mu^{scr}(R_{\mu\nu},\{N_{\mu i}^0\}) = \\ = Z_\mu - \sum_i N_{\mu i}^0[1-\alpha_{\mu i}\exp(-\alpha_{\mu i}R_{\mu\nu}/R_{\mu i}^0)]\,, \quad (2)$$

$$Q_\mu = Z_\mu^{scr}(R_{\mu\nu},\{N_{\mu i}^0\}) - Z_\mu^{scr}(R_{\mu\nu},\{N_{\mu i}\})\,, \quad (3)$$

are screened nuclear and nonpoint ionic charges, respectively; Z_μ is the charge of the μ^{th} nucleus plus core electrons; $R_{\mu\nu}$ is the internuclear distance; $R_{\mu i}^0 = n_{\mu i}/\xi_{\mu i}^0$ is the most probable distance between the i^{th} electron and the corresponding μ^{th} nucleus, $n_{\mu i}$ and $\xi_{\mu i}^0$ are the principal quantum number and Slater exponent of i^{th} atomic orbital (AO) centered at the μ^{th} nucleus; E_μ^0 and E_μ are the total energies of individual atoms in non-interacting and interacting systems characterized by sets of occupancy numbers $\{N_{\mu i}^0 \equiv P_{\mu i,\mu i}^0\}$ and $\{N_{\mu i} \equiv P_{\mu i,\mu i}\}$ and energies $\{E_{\mu i}^0\}$ and $\{E_{\mu i}\}$ of valence AOs, respectively; α and a are fitting parameters. Q_μ, $P_{\mu i,\nu j}$ and $H_{\mu i,\nu j}$ are the non-point charge of the atoms, bond order matrix, and Hamiltonian matrix, respectively.

A secular equation $\sum_{\nu j}(H_{\mu i,\nu j} - \varepsilon\delta_{\mu i,\nu j})C_{\nu j} = 0$ is solved self-consistently to obtain electronic spectra $\{\varepsilon_k\}$ and AO expansion coefficients $\{C_{\nu j}(k)\}$ of the molecular orbitals (MO) of the system. AOs are defined such that they are orthogonal.

NTB uses a new definition of the repulsive energy term with simple physical content; it is the sum of the repulsion energy between nuclei and half of the attraction energy of electrons to "foreign" nuclei. In NTB, this term (the first term in (1) in the non-self-consistent calculation case), unlike that in traditional TB, does not contain the complex interatomic electron-electron interaction energy even implicitly, and thus can be represented more reliably by short-range pairwise functions of interatomic distances. Moreover, accurate and detailed parameterization of ionization and promotion energies of atoms and ions is one of the principal differences of NTB from traditional TB models, enabling one to account adequately for the majority of correlation effects in multiatomic systems as well. AO energies, depending on the charge and excited states of atoms were parameterized with six parameters fit to the electron transition energies between high-spin states of the silicon atom and ion. Repulsive and ion-ionic parts include 4 parameters. NTBM matrix elements include 16 parameters, 4 parameters for each type of matrix element (ss, sp, pp-σ, pp-π). All 20 parameters have been fitted to the following data on small silicon Si_n clusters where $2 \le n \le 7$ [31]: 1) experimental bond lengths [32], bond energy, frequency, adiabatic ionization potential (IP) [33] and electron affinity (EA) [34] of Si_2, bond lengths of the Si_2^+ cation and Si_2^- anion calculated by the MP2(full)/6-311G(3df, 2p) method (2.258 Å and 2.118 Å respectively); 2) experimental cohesion energies [35] of Si_n where $3 \le n \le 7$, excepting Si_5 for which the G2 theoretical result was accepted [36]; 3) geometry of Si_n where $3 \le n \le 7$, obtained by the MP2/6-31G* method [37] and specified with 2 geometrical parameters in each case (Fig. 1): by 2 equal bond lengths and angle between them for Si_3, by length of edge and short diagonal of rhombus for Si_4, by distance between apex atoms and edge of bases of the equilateral polygon of the trigonal (D_{3h}), tetragonal (D_{4h}) and pentagonal (D_{5h}) bipyramids for Si_5, Si_6, and Si_7 correspondently. For other formulae and details of NTB see Ref. [25].

Molecular Dynamics (MD) was used here for determination of the possible spatial structures. It was based on numerical integration of Newton's equations [38]:

$$m_i\frac{d^2r_i}{dt^2} = m_i a_i = F_i \qquad F_i = -dU/dr_i \quad (4)$$

where m_i, r_i and a_i are mass, position and acceleration of the i^{th} particle, respectively; F_i is the total force exerted on the i^{th} particle by all other particles; and U is the total potential energy of the system, which can be computed by one of the approximation methods.

The MD method employed here actually performs minimization of the many variable function, i.e. it minimizes the total energy of the system (locally) by varying the coordinates of atoms following Newton's laws, with occasional damping by removal of kinetic energy from the system. This can also be done by other well-known numerical methods, such as the conjugate gradient method. However the MD approach has several advantages. For example, it is algorithmically simple to realize, and it naturally differentiates light and fast particles from heavy and slow ones which is helpful in avoiding some undesirable and non-physical situations.

To define the cluster configurations that are local and global minima, one must construct an initial geometry from which to start the MD. While it is possible that the intuitively chosen initial geometry could be close to a local (or the global) minimum, this is unlikely. Thus, atoms will exert forces on each other and will move from their initial positions towards new ones which correspond to a lower potential energy. Then kinetic energy of the system will increase as the potential decreases. The kinetic energy is tracked, and when there is a time-step during which it decreases (indicating that the potential energy has increased), kinetic energy is removed from the system, quenching it near a local minimum. This dissipation is repeated as the system oscillates around the local minimum, being forced closer to it each time that the kinetic energy is removed. The simulation is ended when the kinetic energy of the system remains sufficiently small. Note that the same dissipation occurs in real clusters as they cool, exchanging energy with the surrounding gas or, via radiation, with solid surfaces. The calculation is repeated for different initial configurations of the clusters and the stable and metastable structures are determined by comparing total energies of the cluster geometries obtained with the given number of atoms.

3. RESULTS AND DISCUSSIONS

Known equilibrium geometries of the small clusters [39] (Fig. 1) were chosen as the initial configuration for all models. Optimization of the geometry was carried out without constraining the point-group symmetry of

the clusters. As a criterion for the existence of a bond between atoms we chose the separation distance of $R = 2.80$ Å. This value was also used in Ref. [40] Charged states have been studied by adding or removing electrons, either by elimination of an electron from the highest occupied molecular orbital (HOMO) or by addition of the electron to the HOMO (if it is partially filled in the neutral cluster) or to the lowest unoccupied molecular orbital (LUMO). Self-consistent calculations provided the effective distribution of the charge among the atoms. For comparing different charged states of the clusters, the cohesion energy per atom was calculated with the following correction:

$$E = E_{total} \pm E_{corr}\,, \qquad (5)$$

where E_{corr} – correction for electron affinity or ionization potential of the atom. It is needed to restore the initial, calculated value of the binding total energy, because of E_{total} is value applied from the energy of the isolated atoms and ions, i.e. an ionization potential or electron affinity of the corresponding element of the cluster was added (or subtracted) in the case of charged clusters.

Obtained results on the ground-state equilibrium structures for the small neutral and ionic Si_3-Si_8 clusters are displayed in Fig. 2.

Comparison of the properties of small silicon clusters containing from 2 up to 7 atoms is resulted in Tables 1 and 2. As seen the stable isomers for Si_4 is not only the rhombic form but also trigonal, tetragonal and pentagonal bipyramids that corresponds to results of ab initio calculations and experiments. NTBM results for cohesive energy coincide with results of theory G_2, DMC, density functional theory (DFT), GGA (except for Si7).

The calculated bond lengths are in a good agreement with results of non-empirical calculations although have weak underestimation (0,01-0,04 Å) of the bond lengths.

Neutral and negative charged silicon dimer is investigated by Curtiss and et al. [21]. Along with these charged clusters also positive and double positive charged dimers are calculated by us. At changing of a charge states the atoms in a negative states close to each other, in positive one they repulse and remove from each other. Atom repulsion in a positive charged molecule occurs because of increasing of Madelung component in total energy expression.

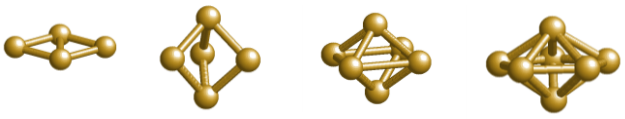

Fig. 1 – Equilibrium geometries of the small clusters

3.1 Si_3

The Si_3 cluster had an isosceles triangle geometry with C_{2v} symmetry, in all cases except for the double positively charged state (Fig. 2). The Si_3^{++} cluster had the high symmetry (C_{3v}) equilateral triangle configuration. Interatomic distances decreased in negatively charged clusters compared to the neutral one (Table 1).

To understand the nature of the bonding in Si_3, the charge allocation on the valence *s*- and *p*-orbitals in

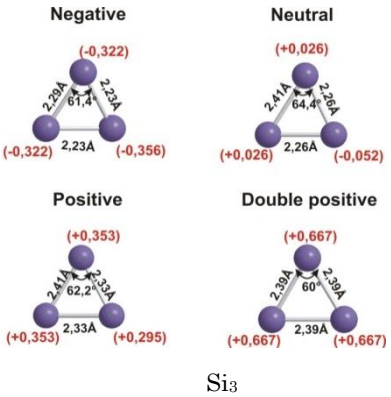

Si_3

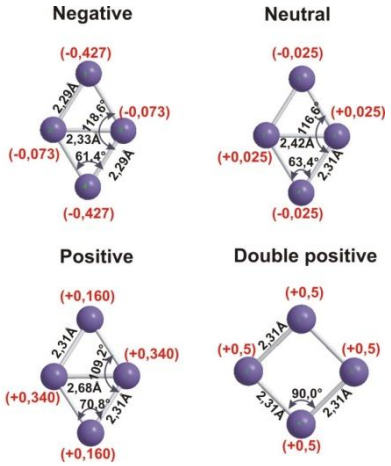

Si_4

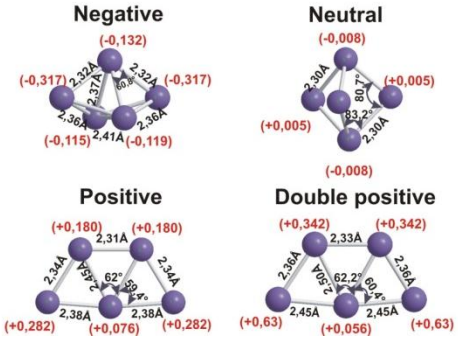

Si_5

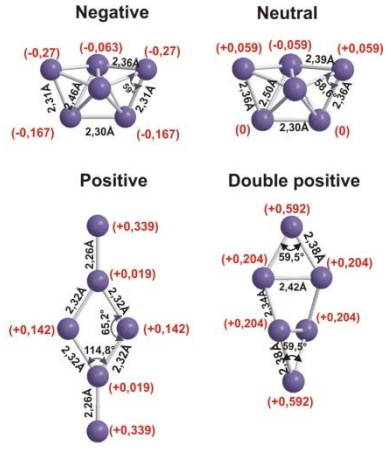

Si_6

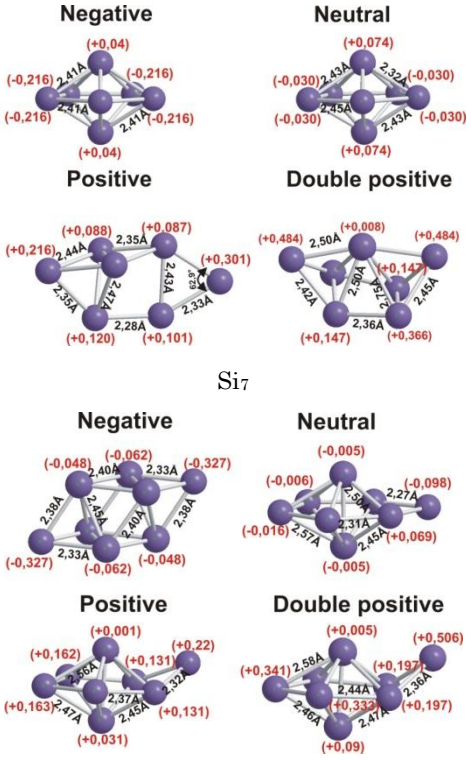

Fig. 2 – Ground-state equilibrium geometries for the neutral and ionic small Si3-Si7 clusters (silicon atoms are displayed by dark circles, the lines are chemical bonds between them, the red color numbers in parenthesis are partial charges on the atoms, black color numbers show bond length in angstrom, bond angles values are accompanied by arrows

different charge states of the cluster have been analyzed. In the case of Si_3^0 the hybridizations of the valence orbitals are $s^{1.59}p^{2.46}$ and $s^{1.77}p^{2.21}$ for the apical and other atoms, respectively ($s^{1.64}p^{2.36}$ and $s^{1.94}p^{2.06}$ were found by Raghavachari and Rohlfing [41]). There are two different hybridization types of these atoms, in contrast to the other charge states where the cluster has an equilateral high symmetry configuration and all atoms have identical hybridization. These were $s^{1.7}p^{2.62}$, $s^{1.73}p^{1.93}$ and $s^{1.75}p^{1.58}$ hybridizations for Si_3^-, Si_3^+ and Si_3^{++}, respectively. As shown in Table 2, the binding energy between the apical atom and each of the other atoms is considerably greater than the binding energy between the side atoms (connected by a longer bond). Bond order matrix analysis shows that the valence orbital of the atoms has sp^2 hybridization in the charged states and π-bond exists between overall atoms. Distortion of the high symmetrical configuration with symmetry lowering may be caused by either change of the valence orbital hybridization of one of the atoms from sp^2 to sp^3 or by instability of the high symmetry related to an approximate functional form of the single Slater determinant assumed for the wave function. In the latter case, energy optimization may lead to a function that does not have pure symmetry and does not transform like any irreducible representation under the operations of the group. Such imperfection is also typical of ab-initio Hartree-Fock calculations [43].

The fact that the cohesion energy per atom for the neutral cluster is lower than for the positive and negatively charged ones is explained by the delocalization of the charge over the π-ring. In the case of Si_3^{++} which has the equilateral triangle geometry, the Highest Occupied Molecular orbital (HOMO) is degenerate with the Lowest Unoccupied Molecular Orbital (LUMO). The lengthening of the Si-Si bond upon removal of electrons results from increasing ion-ionic interaction between atoms. In the doubly charged state, the Madelung part of the total energy which corresponds to the ion-ion interaction sharply increased as seen from Table 3.

3.2 Si_4

The most energetically favorable structure for Si_4 had the form of the planar rhombus (Fig. 3A) with D_{2h} symmetry, in all cases except for the double cation. Short-length opposite atoms formed a chemical bond. The cohesion energy per atom of this structure for the neutral cluster was 0.348 eV greater than for the next less stable structure (Fig. 3B). Our results are in good agreement with ab-initio calculations [21]. The difference between bond lengths obtained by us and the results given by Curtiss et al (2.31 Å and 2.41 Å) [21] are as small as 0.01 Å for the neutral cluster and 0.02 Å for the negatively charged system (2.30 Å and 2.35 Å) [21]. As shown in Fig. 2, with increasing positive charge on the cluster, the sharp angles of the rhombus were increased whereas the obtuse angles were decreased, such that the rhombus configuration transformed smoothly to a rectangular one and acquired the form of a planar square (D_{4h} symmetry) for the double positively charged state. The diagonal bond was broken in this case, and the four atoms were equivalent. Bond order matrix analysis shows that all bonds including the diagonal bond were σ-bonds. The electronic charge density was moved to the long-length opposite atoms in the rhombus-like clusters.

Table 1 – Cohesive energies (in eV) of small silicon clusters

Clusters	MP4/6-31G* [25]	MP2/6-31G(d) [26]	G2 theory [24]	LDA [22]	GGA [22]	DMC [23]	NTB [our work]	TB [11]	Expt [23]
Si_2	1.30	1.29	1.60	1.97	1.76	1.58	1.599	1.60	1.61
Si_3	2.11	2.15	2.47	2.93	2.54	2.37	2.51	2.51	2.45
Si_4	2.64	2.74	2.99	3.51	3.04	2.86	3.03	3.21	3.01
Si_5	2.75	–	3.23	3.79	3.27	–	3.22	3.16	–
Si_6	3.00	3.18	3.45d	4.00	3.44	3.26	3.48	–	3.42
Si_7	3.17	3.31	–	4.15	3.56	3.43	3.65	–	3.60

Table 2 – Characteristic bond distances (in Å) for small silicon clusters calculated by different methods

Clusters	Characteristic bond distances	MP2/6-1G* [25, 25]	NTBM [our work]	TB [19]	DFTB [15]
Si_3 (C_{2v})	R(1–2) R(1–3) R(3–4)	2.191[a] 2.806[a]	2.263 2.264 2.416	2.28 2.71	2.221 2.972
Si_4 (D_{2h})	R(1–2) R(1–3) R(3–4)	2.312 2.413	2.306 2.423	2.34 2.54	2.313 2.659
Si_5 (D_{3h})	R(1–2) R(1–3) R(3–4)	3.057 2.296 2.967	3.057 3.035 2.983	2.94 2.36 3.20	3.119 2.331 2.959
Si_6 (–)	R(1–2) R(1–3) R(3–4)	2.694 2.356 2.734	2.387 2.364 2.301		
Si_7 (D_{5h})	R(1–2) R(1–3) R(3–4)	2.512 2.457 2.483	2.506 2.431 2.449		2.858 2.658 2.634

[a]Results at the QCISD(T)/6-31G* level of theory.

Table 3 – Cohesion energy per atom and bond distances for silicon dimer

Charge state	Cohesion energy per atom, eV	RSiSi, Å, [our]	RSiSi, Å, [24]
Si^2	1.5994	2.2155	2.260
Si^{-2}	2.0161	2.1295	2.124
Si^{+2}	1.7257	2.2935	
Si^{++2}	– 1.4188	2.2790	

Table 4 presents a comparison of the cohesion energies per atom of the Si_4 clusters in different charge states. The neutral cluster is less stable than other singly charged states. The negatively charged Si_4 is the most stable state. However, all three clusters, Si_4^-, Si_4^0 and Si_4^+, have similar cohesion energies, within 0.17 eV. The doubly-charged Si_4^{++} has significantly smaller cohesion energy.

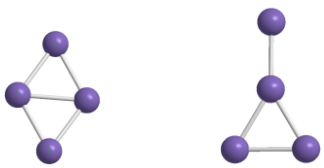

A B

Fig. 3 – Ground equilibrium geomtries of the Si_4 cluster: the most favorable configuration (3,0315 eV) (A); the second stable configuration (2,6937 eV) (B)

3.3 Si_5

The Si_5 cluster takes the form of a trigonal bipyramid with D_{3h} point symmetry in the neutral state (Table 5). The bond lengths are 2.98 Å therein. The bond angles are equal to 80.7° which is significantly less than 109°27', the angle characteristic of ideal sp^3-hybridization. The charge states of the atoms were near zero. In the negative state, interatomic distances increased as the symmetry decreased from D_{2h} to C_{2v}. Moreover, the apex atoms were displaced from their symmetrical positions, producing a non-planar rhombus structure. Most of the charge was allocated on these apical atoms. The cohesion energy per atom calculated here coincides with the results of ref [23] to within 0.01 eV.

Table 4 – Cohesion energy per atom for Si4 cluster in different charge states

	Si_4^-	Si_4^0	Si_4^+	Si_4^{++}
Point group of symmetry	D_{2h}	D_{2h}	D_{2h}	D_{4h}
Cohesion energy per atom, eV	3,215	3,0315	3,087	1,87

For the positively charged state a planar form was the most energetically favorable structure, in agreement with Raghavachari's work [37-38]. Once again, charge localization on the terminal atoms is predicted. Note that the positively charged cluster has the form of a half hexagon constructed from planar triangles. Despite this planarity, which might suggest π-bonding, bond order matrix analysis shows only σ-bonds between the atoms. The doubly positively charged state has a planar geometry similar to the singly-charged state, but with longer bond-lengths. The cohesion energy per atom was similar in the neutral and singly-charged clusters, with the anion the most stable, while the doubly-positively charged cluster had much smaller cohesion energy.

Table 5 – Cohesion energy per atom for Si_5 cluster in different charge states

	Si_5^-	Si_5^0	Si_5^+	Si_5^{++}
Point group of symmetry	C_{2v}	D_{3h}	C_2	C_2
Cohesion energy per atom, eV	3.46	3.22	3.26	2.41

3.4 Si_6

The most stable configuration for the neutral Si_6 cluster was the "boat" form (Fig. 2) based. The nonplanar rhombus that constitutes the upper rim of the boat had acute and dihedral angles of 62.2° and 18.7°, respectively. The interatomic distances for the bonds in this nonplanar rhombus were 2.39 Å. The bond length between the two other atoms was 2.30 Å, and these atoms were bound to the apical atoms of the boat at a distance of 2.36 Å. There is slight charge redistribution among the atoms of the rhombus making up the rim of the boat, while the other two atoms remain neutral.

In the negatively charged state, the bond lengths were shorter than for the neutral cluster. The acute angles of the rhombus decreased to 59.4°. Its dihedral angle was changed slightly to 18.3°. Most of the charge was allocated on the apical atoms of the boat. The positively-charged Si_6^+ cluster assumed a planar form with D_{2h} symmetry (Table 6). The central rhombus had acute angles of 65.1°. This can be viewed as a result of the breaking of the bond making up the base of the boat. The Si_6^{++} dication assumed a twisted from that retained D_2 symmetry. The dihedral angles between bonds of the central tetragon was 47.5°. The terminal

atoms of the cluster were each bonded with two atoms of the tetragon. The positive charge was again localized on the apical atoms.

Table 6 – Cohesion energy per atom for Si6 cluster in different charged states

	Si_6^-	Si_6^0	Si_6^+	Si_6^{++}
Point group of symmetry	C_{2v}	C_{2v}	D_{2h}	D_2
Cohesion energy per atom, eV	3.66	3.48	3.42	3.33

The cohesion energy per atom in the different charge states of the Si_6 decreased monotonically with removal of electrons. Analysis of the bond matrix showed that the positively charged Si_6 cluster had π-bonding distributed over the cluster, consistent with the observation that the interatomic distances in this state were shorter than in the others.

3.5 Si_7

The neutral Si_7 cluster has the form of a pentagonal bipyramid with D_{5h} symmetry where two atoms, apex and bottom, are placed above and below the planar pentagon basis constructed from five silicon atoms (Table 7). The lengths of the bonds between apex and base atoms are different and vary from 2.32 Å to 2.43 Å. The bond lengths between the atoms in the pentagonal base are longer, at 2.43 Å.

The anion had the same pentagonal bipyramidal configuration, but the apical atoms were placed symmetrically and all bonds between them and the base had the same length, 2.41 Å. The negative charge localized on the atoms of the pentagonal base, while the apical atoms remained slightly positively charged.

Removal of an electron from the neutral Si_7 cluster led to rearrangement to a lower symmetry structure, made up of a planar rhombus and perpendicular to it a planar combination of a quadrangle and triangle. Point symmetry of the cluster changed from D_{5h} in the neutral cluster to C_{2v} in the positive state. The positive charge was allocated mostly to the terminal atoms of the cluster, as for the smaller clusters.

Table 7 – Cohesion energy per atom for Si_7 cluster in different charged states

	Si_7^-	Si_7^0	Si_7^+	Si_7^{++}
Point group of symmetry	C_{5v}	C_{5v}	C_{2v}	C_{2v}
Cohesion energy per atom, eV	3.80	3.65	3.59	3.06

The dication takes the form of a bath-tub or boat-like structure constructed from six silicon atoms with a seventh atom above it. However the bath-tub is slightly non symmetric and as a result, the charge distributed irregularly among the atoms on the bottom of the bath-tub.

3.6 Si_8

A distorted tetragonal prism configuration with C_{2h} point symmetry group was found to be the most stable for the anionic Si_8 cluster (Table 8). In contrast, the neutral cluster had the form of a hexagonal bipyramid. Its basis is planar but not regular and has a three different values of bond lengths (2.27 A, 2.31 A, 2.36 A). In the singly positive state the symmetry of the cluster is broken and the short-distanced atom of the base were displaced up from the base by about 50°. The second positive charge increased this angle up to 55°. This atom apparently is the additional one to the Si_7 cluster because geometry of the Si_7 is kept in Si_8. Distance between atoms becomes longer on negative state and shorter on positive and double positive ones. The nearest opposite sides of the bipyramid basis become further from each other and the basis broadened (~ 0.15 A) from the neutral cluster through dication.

The charges of two apex atoms are nearly neutral in all charged states. But non-planar atom of the basis is the most sensitive to the charge variations.

Zhu and Zheng [23] found by ab-initio MP2/6-31G(*d*) calculations that a distorted octahedron as the most stabile form of neutral Si_8 and the structure like one given here as a configuration with a local minima. But most of bond lengths is longer (~ 0.1 A) there than our's. DFT calculations with BLYP and BP86 proceed by Yang et al [44] show that a neutral Si_8 changes its geometry with C_{2h} symmetry to the isomer with C_{3v} in its anion. There are no experimental values for comparison these results.

Table 8 – Cohesion energy per atom for Si8 cluster in different charged states

	Si_8^-	Si_8^0	Si_8^+	Si_8^{++}
Point group of symmetry	C_{2v}	C_{2v}	C_{2v}	C_{2v}
Cohesion energy per atom, eV	3.84	3.68	3.77	3.30

4. CONCLUSION

Application of the NTBM to research the different charge states of the small bare clusters of silicon shows a competitive accuracy of the results with the data obtained from different ab-initio HF and DFT methods.

For all Si_3-Si_8 clusters, closed triangular structures and spatial figures based on triangles are the most stable configurations in neutral and negative states because of the effect of the strong overlapping of the free valence atomic orbitals of silicon. The neutral and negatively charged states have a similar spatial structure in all clusters. This can be explained by the closeness of their Madelung interaction between atoms as shown in Fig. 4. This also shows that the ion-ionic interaction is stronger in the case of a positive charge than for of a negative one.

Th Anderson *U*(-) effect, i.e. instability of the neutral structure in comparison with negative and positive charge states is observed in small Si_2-Si_5 and Si_8 clusters. This can be explained by the fact that the cluster consisting 6 or 7 atoms is most compacted and atoms in it are most saturated by bonding to each other having highest coordination number among other clusters. This led Si_6 and Si_7 clusters in neutral charge state to be marked amongst other clusters for their unusual stability. Attachment and detachment of an electron means to occur in pairs for these clusters and cluster changes its charge from negative to positive at once

and vice versa but these becomes less with increasing of the amount of Si atoms in the cluster due to small difference of energies between for the neutral and positive clusters (0.13 eV). Such a trend is not observed in the Si_6 and Si_7 clusters. At the same time, as shown in the picture, double positive states are the most energetically stable for all clusters though it gets closer to other charged states for the cluster, containing six silicon atoms as seen from Fig. 5.

The geometrical configurations of small silicon clusters found by us, except for Si_7, coincide with the figures resulted in works Yoo and Zeng [41], and in ref [23] as well.

ACKNOWLEDGEMENTS

The research described in this publication was made possible in part by Uzbek Academy Sciences Fund for Supporting Fundamental Research and US CRDF grant award (No UZC2-2877-TA-07).

REFERENCES

1. H. Shiromaru, T. Moriwaki, H. Ikeda, Y. Achiba, *Zeitschrift fur Physik D* **26**, 216 (1993).
2. O. Cheshnovsky, S.H. Yang, C.L. Pettiette, M.J. Craycraft, Y. Liu, R.E. Smalley, *Chem. Phys. Lett.* **138**, 119 (1987).
3. J.R. Heath, Y. Liu, S.C. O'Brien, Q.L. Zhang, R.F. Curl, F.K. Tittel, R.E. Smalley, *J. Chem. Phys.* **83**, 5520 (1985).
4. M.L. Mandich, W.D. Reents, Jr., V.E. Bondybey, *J. Phys. Chem.* **90**, 2315 (1986).
5. M.L. Mandich, V.E. Bondybey, W.D. Reents, Jr., *J. Phys. Chem.* **86**, 4245 (1987).
6. J.L. Elkind, J.M. Alford, F.D. Weiss, R.T. Laaksonen, R.E. Smalley, *J. Chem. Phys.* **87**, 2397 (1987).
7. W.R. Creasey, A. O'Keefe, J.R. McDonald, *J. Phys. Chem.* **91**, 2848 (1987).
8. M.F. Jarrold, J.E. Bower, K. Creegan, *J. Chem. Phys.* **90**, 3615 (1989).
9. M.F. Jarrold, J.E. Bower, *J. Phys. Chem.* **92**, 5702 (1988).
10. L.A. Bloomfield, R.R. Freeman, W.L. Brown, *Phys. Rev. Lett.* **54**, 2246 (1985).
11. Y. Liu, Q.L. Zhang, F.K. Tittel, R.F. Curl, R.E. Smalley, *J. Chem. Phys.* **85**, 7434 (1986).
12. Q.L. Zhang, Y. Liu, R.F. Curl, F.K. Tittel, R.E. Smalley, *J. Chem. Phys.* **88**, 1670 (1988).
13. Th. Frauenheim, F. Weich, T. Kohler, S. Uhlmann, D. Porezag, G. Seifert, *Phys. Rev. B* **52**, 11492 (1995).
14. T.J. Lenosky, J.D. Kress, I. Kwon, A.F. Voter, B. Edwards, D.F. Richards, S. Yang, J.B. Adams, *Phys. Rev. B* **55**, 1528 (1997).
15. K. Stokbro, N. Chetty, K.W. Jacobsen, J.K. Norskov, *Phys. Rev. B* **50**, 10727 (1994); P. Horsfield, A.M. Bratkovsky, M. Fearn, D.G. Pettifor, M. Aoki, *Phys. Rev. B* **53**, 12694 (1996).
16. K. Colombo, *Annual Rev. Computational Phys., Vol. IV* (Ed by D. Stauffer) (World Scientifc: Singapore: 1996); A. Sieck, D. Porezag, Th. Frauenheim, M.R. Pederson, K. Jackson, *Phys. Rev. A* **56**, 4890 (1997).
17. L.J. Lewis, N. Mousseau, *Comput. Mater. Sci.* **12**, 210 (1998); G. Galli, *ibid.* **12**, 242 (1998).
18. C. Xu, T.R. Taylor, G.R. Burton, D.M. Neumark, *J. Chem. Phys.* **108**, 1395 (1998).
19. B. Liu, Z.Y. Lu, B. Pan, C.Z. Wang, K.M. Ho, A.A. Shvartsburg, M.F. Jarrold, *J. Chem. Phys.* **109**, 9401 (1998).
20. J.C. Grossman, L. Mitas, *Phys. Rev. Lett.* **74**, 1323 (1995).
21. L.A. Curtiss, P.W. Deutsch, K. Raghavachari, *J. Chem. Phys.* **96**, 6868 (1992).
22. K. Raghavachari, C.M. Rohlfing, *J. Chem. Phys.* **89**, 2219 (1988); K. Raghavachari, C.M. Rohlfing, *J. Chem. Phys.* **96**, 2114 (1992).
23. X.L. Zhu, X.C. Zeng, *J. Chem. Phys.* **118**, 3558 (2003).
24. K. Raghavachari, V. Logovinsky, *Phys. Rev. Lett.* **55**, 2853 (1985).
25. Z.M. Khakimov, *Comput. Mater. Sci.* **3**, 95 (1994).
26. P.L. Tereshchuk, Z.M. Khakimov, F.T. Umarova, M.T. Swihart, *Phys. Rev. B* **76**, 125418 (2007).
27. Z.M. Khakimov, F.T. Umarova, A.P. Mukhtarov, *Appl. Sol. Energ.* **6**, 19 (1994).
28. Z.M. Khakimov, A.P. Mukhtarov, A.A. Levin, *FTP* **28**, 571 (1994). (*Semiconductors* **28**, 344 (1994)).
29. Z.M. Khakimov, A.P. Mukhtarov, F.T. Umarova, A.A. Levin, *FTP* **28**, 1727 (1994). (*Semiconductors* **28**, 959 (1994)).
30. A.P. Mukhtarov, D.S. Pulatova, N.T. Sulaymonov, Z.M. Khakimov, *FTP* **28**, 1015 (1994). (*Semiconductors* **28**, 587 (1994)).
31. Z.M. Khakimov, P.L. Tereshchuk, N.T. Sulaymanov, F.T. Umarova, M.T. Swihart, *Phys. Rev. B* **72**, 115335 (2005).
32. *Molekularniye konstanti neorganicheskih soedineniy. Spravochnik* (Ed. by K.S. Krasnova) (Moskva: Khimiya: 1979).
33. B. Liu, Z.Y. Lu, B. Pan, C.Z. Wang, K.M. Ho, A.A. Shvartsburg, M.F. Jarrold, *J. Chem. Phys.* **109** No 12, 9401 (1998).
34. C. Xu, T.R. Taylor, G.R. Burton, D.M. Neumark, *J. Chem. Phys.* **108** No 4, 1395 (1998).
35. J.C. Grossman, L. Mitas, *Phys. Rev. Lett.* **74**, 1323 (1995).
36. L.A. Curtiss, P.W. Deutsch, K. Raghavachari, *J. Chem. Phys.* **96** No 9, 6868 (1992).
37. K. Raghavachari, C.M. Rohlfing, *J. Chem. Phys.* **89** No 4, 2219 (1988).
38. M.P. Allen, D.J. Tildesley, *Computer simulation of liquids* (Oxford: Clarendon Press: 1987).
39. Cunyuan Zhao, K. Balasubramanian, *J. Chem. Phys.* **116**, 3690 (2002).
40. S. Yoo, X.C. Zeng, *J. Chem. Phys.* **119**, 1442 (2003).
41. K. Raghavachari, C.M. Rohlfing, *J. Chem. Phys.* **96**, 2117 (1992).
42. Sieck, Th. Frauenheim, K.A. Jackson, *phys. status solidi b* **240**, 537 (2003).
43. E.R. Davidson, W.T. Borden, *J. Phys. Chem.* **87**, 4783 (1983).
44. J.C. Yang, W.G. Xu, W.S. Xiao, *J. Molec. Struc.: Theochem.* **719**, 89 (2005).